Spherical Mapping: A Powerful Tool for 3D Object Matching

Danco Davcev
Ss. Cyril and Methodius University in Skopje

Vladimir Trajkovik
Ss. Cyril and Methodius University in Skopje

Slobodan Kalajdziski
Ss. Cyril and Methodius University in Skopje

SETIT 2007
4th International Conference: Sciences of Electronic,
Technologies of Information and Telecommunications
March 25-29, 2007 – TUNISIA

Spherical Mapping: A Powerful Tool for 3D Object Matching

Blerim Mustafa, Danco Davcev, Vladimir Trajkovik, Slobodan Kalajdziski

Faculty of Electrical Engineering, University Sts. Cyril and Methodius, Karpos II bb, Skopje, Macedonia

blerim.mustafa@mt.com.mk
etfdav@etf.ukim.edu.mk
trvlado@etf.ukim.edu.mk
skalaj@etf.ukim.edu.mk

Abstract: Matching 3D objects by their similarity is a fundamental problem in computer vision, multimedia databases, molecular biology, computer graphics and a variety of other fields. A challenging aspect of this problem is to find a suitable shape signature/descriptor that can be constructed and compared quickly, while still discriminating between similar and dissimilar shapes.
We find that the major problems in comparing 3D mesh objects lie in the non-uniform vertex sampling and level of detail distribution, in the non-uniform polygon topology and in mesh-representation anomalies, so the primary motivation behind the work presented in this paper is the introduction of mesh-parameterization which brings meshes into a form having uniform vertex sampling, uniform polygon topology and filtered anomalies, by spherically mapping the mesh surface.
Further, we present two approaches in inferring shape-descriptors from the spherically mapped objects and the results from the conducted experiments.
Key words: 3D Object matching, spherical harmonics, discrete wavelet transform, MPEG7 descriptor.

INTRODUCTION

Determining the similarity between 3D shapes is a fundamental task in shape-based recognition, retrieval, clustering, and classification. Its main applications have traditionally been in computer vision, mechanical engineering, and molecular biology.

However, we believe that 3D object databases will become ubiquitous and the applications of 3D shape analysis and matching will expand to a wide variety of other fields, due to several recent rapid developments:

- The development of the 3D model acquisition tools (modeling applications and 3D scanners),
- The development of fast and cheap high-end 3D graphics hardware,
- The development of large publicly-available 3D databases (Protein Database, for instance).

Representing and processing 3D models is more complicated than the traditional sampled multimedia data (sound, image and video). The main difficulty is that 3D surfaces rarely have simple parameterizations, that is, they have:

- Non-uniform vertex sampling and level of detail distribution,
- Non-uniform polygon topology.

Since 3D surfaces can have arbitrary topologies, many useful methods for analyzing other media (e.g., Fourier analysis) have no obvious analogs for 3D surface models. Moreover, the dimensionality is higher, which makes searches for pose registration, feature correspondences, and model parameters more difficult, while the likelihood of model anomalies is higher. In particular, most 3D models in large databases are represented by “polygon meshes” – unorganized and degenerate sets of polygons. They seldom have any topology or solid modeling information; they rarely are manifold; and most are not even self-consistent. Practically, every 3D computer graphics model available today contains missing, wrongly-oriented, intersecting, disjoint, and/or overlapping polygons.

The problem of determining the similarity of two shapes has been well-studied in several fields. For a broad introduction to shape matching methods, please refer to any of several survey papers, such as [1]. Roughly, the methods can be divided in several classes. The first class contains the methods based on calculating statistical features of the 3D objects. The descriptors proposed by Paquet and Rioux, based on abstractly defined moments and cords [8] and the shape distribution descriptor by Osada and Funkhouser [7] are typical examples of this class. The second class is the class of methods based on geometry features of the 3D object. Suzuki proposes the method of equivalence classes [10]. The MPEG-7 shape spectrum descriptor [5, 6] is also a representative approach of this class. The third class compiles the approaches based on the topology features, such as the descriptor based on the Reeb-graph [4]. Finally, the fourth class compiles the methods based on binary voxel grids, which analyze binary voxelised models rather than working directly with 3D meshes. Kazhdan and Funkhouser's descriptors [2] are typical representatives of the class.

To summarize, many of these approaches have difficulty with 3D polygon meshes because they invariably require leaning on at least one of the following difficult assumptions: the mesh is clear of anomalies, the mesh has an almost uniform distribution of level of details, the compared meshes have same/similar polygon count etc. The motivation behind our work is to develop a fast, simple, and robust method for matching 3D polygonal models without relying on these hard assumptions.

The remainder of the paper is organized as follows. An overview of the proposed approach with detailed descriptions of issues and proposed implementing appear in section 1. Section 2 presents results of experiments aimed at evaluating the robustness and discrimination power of the proposed approach. Finally, section 3 contains a summary of our experiences.

1. Overview of Approach

The main idea behind the development of the sphere mapping scheme for 3D object matching is to solve one of the biggest problems in the field, which is the non-uniform sampling of vertices and the difference in polygon topology among separate mesh-objects. Vast majority of the existing methods for matching 3D objects by similarity would have problems in matching two practically same objects if they have different levels of tessellation, different vertex positioning, or even different polygon connectivity.

That is why we decided to introduce a preprocessing parameterization scheme, which outputs a mesh with uniform (parameterized) topology. Figure 1 illustrates this scheme; MxN segment sphere is placed around the object, and the sphere-vertices are radially collapsed towards the sphere center until they touch the mesh surface.

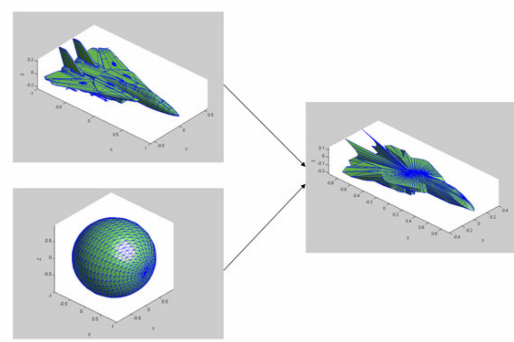

Figure 1. *Sphere mapping scheme.*

Mesh-object I is normalized to a unit bounding box around the coordinate center and a sphere Ω with radius $r=1$ is placed on the coordinate center (surrounding the mesh object I). Then, we define a set of rays $u(\theta,\varphi)$ $(\theta=[0,\pi],\varphi=[0,2\pi])$, starting at the center of the sphere and with a heading defined by the angles θ and φ. A function $f(\theta,\varphi)$ is than defined on the sphere Ω :

$$f(\theta,\varphi)=\max\{\{0\}\cup(|u(\theta,\varphi)\cap I|)\} \quad (1)$$

The function $f(\theta,\varphi)$ is sampled with $4B^2$ equiangular samples $f_{ab}(0\le a,b\le 2B-1)$, such that:

$$\theta_a=\frac{2a+1}{4B}\pi,\varphi_b=\frac{2b\pi}{2B} \quad (2)$$

These samples (f_{ab}) define the vertices (geometry) of the parameterized approximation:

$$\begin{aligned} x_{ab} &= f_{ab}\sin\theta_a\cos\varphi_b \\ y_{ab} &= f_{ab}\cos\theta_a \\ z_{ab} &= f_{ab}\sin\theta_a\sin\varphi_b \end{aligned} \quad (3)$$

while their interconnection into polygons (topology) is the same as the one for the surrounding sphere; i.e. the same for all the objects parameterized using this scheme.

1.1. Spherical Harmonics

Although the approach presented was primarily developed as a scheme for preprocessing mesh-objects, the provided parameterized approximations showed up suitable for defining new methods for inferring signatures (descriptors).

Most obviously, the spherical Fourier transform [3, 9] can be applied on the provided $4B^2$ samples, outputting B^2 complex coefficients $\hat{f}_{l,m}(0\le|m|\le l\le B)$. Using the coefficients from the first $\dim$ sub-bands ($\dim$ being the size of the descriptor vector), we define the descriptor as:

$$f_d = (\|f_0\|,..\|f_{\dim}\|), \|f_l\| = \sqrt{\sum_{m=-l}^{l} \left|\hat{f}_{l,m}\right|^2} \qquad (4)$$

This descriptor has the good feature of orientation invariance, that is, the spherical furrier transform should output the same set of coefficients for the same object in a different orientation.

1.2. Planar Mapping

The other approach is to planar map the acquired samples f_{ab}, so that we end up with a 2D height-map (a $2Bx2B$ pixel grayscale image), suitable for applying algorithms from digital image processing. Using n-level 2D discrete wavelet transform (2DDWT), a simple descriptor can be constructed. The $4B^2$ real coefficients of the 2DDWT are sorted by significance (i.e. by sub-bands):

$$W = (w_1..w_m) = 2DDWT\,(\mathrm{Im}) \qquad (5)$$
$$= (a \mid h_1 \mid v_1 \mid d_1 \mid h_2 \mid v_2 \mid d_2 \mid .. \mid h_n \mid v_n \mid d_n)$$

where a is the approximation (0-th band), and h_i, v_i, d_i are the horizontal, vertical and diagonal characteristics of the i-th band. The descriptor is constructed of the first $\dim$ coefficients of W, $\dim$ being the desired size of the descriptor: $f_d = (w_1, w_2..w_{\dim})$.

This descriptor is obviously orientation – dependent. That's why before the feature extraction, we normalize the object's orientation using the Principal Component Analysis (or Karhunen – Loeve Transform), described in [11].

2. Experimental Results

The experiments are conducted using MATLAB and the spherical harmonics library from [9] over a set of 108 experimental models grouped into 15 groups: Boxes (7 objects), Cars (7), Chairs (5), Copters (6), Cones (5), Mugs (9), Droids (5), Spaceships (9), Missiles (8), Planes (11), Spheres (10), Tables (8), Tanks (6), Teapots (5), Tori (7). A sample of each of the groups is shown on figure 3.

The experiments give comparison of the discrimination power in 3d objects matching using the descriptors described in the previous section and four other descriptors:
- **Moments-based descriptor** [8] with length 451.
- **Shape distribution descriptor with D1 function** [7], using 256 surface points, and descriptor length of 64.
- **Shape distribution descriptor with D2 function** [7], using 256 surface points, and descriptor length of 64.
- **Cords-based descriptor** [8] with length of 120 (three histograms with 40 coefficients each).

These descriptors were chosen because they work on the mesh-domain, i.e. they don't use voxelization (like [2] does, for instance).

We used 63x63 segment spheres to create the approximations (figure 4). For the spherical harmonic descriptors, we used a spherical harmonic transform up to the $\hat{L} = 16$ level, which provides 256 coefficients $\hat{f}_{l,m}, l = 0..15, |m| \le l$, having $\hat{f}_{l,m} = \hat{f}_{l,-m}$. Thus, using the 136 unique coefficients $\hat{f}_{l,m}, l = 0..15, m = 0..l$, descriptors of length 16 are inferred as described in section 1.1. For the planar mapping approach the most significant 16 coefficients of the 6-level Haar wavelet transform are used in the descriptor construction. An illustration of the robustness of these two descriptors is shown in figure 5 and 6, where the descriptor-vectors of each group of objects are plotted together.

The similarity metric for calculating the difference between two descriptors f', f'' is the plain Euclidean:

$$diff\,(f', f'') = \|f' - f''\|_2 = \sqrt{\sum_i (f' - f'')^2} \qquad (6)$$

For each of the 6 descriptors we form 108x108 similarity matrix (values are the differences between objects), and threshold it to a binary matrix (values greater than the threshold are replaced with "1" and values less then the threshold are replaced with "0") in order to see how the objects will group. The obvious ideal thresholded similarity matrix is shown in figure 2. The threshold is a value between the maximum and the minimum value of the similarity matrix for which the thresholded matrix is closest to the ideal. Figure 7 shows the similarity matrices (as greyscaled images, where the darker color corresponds to a lower difference) and their thresholded versions of the 6 descriptors we are comparing.

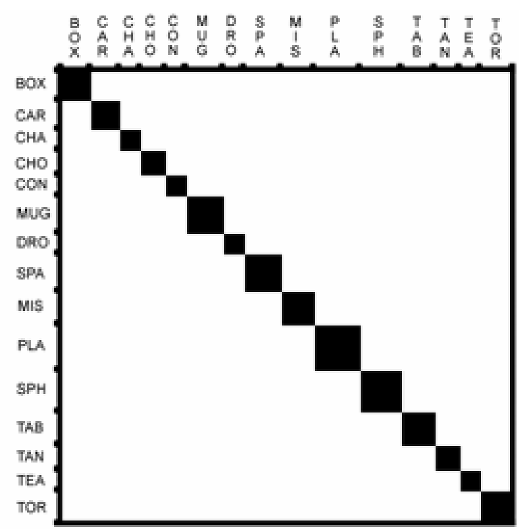

Figure 2. *The ideal similarity matrix would group the objects in the same abstract groups a human would group them.*

We define two quantitative measures to measure the error-rates of the descriptors. If $Ideal_{i,j}$ is the ideal (binary) similarity matrix, $Actual_{i,j}$ is the actual similarity matrix (thresholded to binary), n is the number of test objects (108), gn is the number of groups (15), and $gsize_g$ is the size of the g-th group, we define absolute error as:

$$Err_{Abs} = \frac{\sum_{i=1}^{n}\sum_{j=i}^{n} abs(Ideal_{i,j} - Actual_{i,j})}{n(n+1)} \quad (7)$$

and the relative error (relative to the sizes of the groups of objects) as:

$$Err_{rel} = \frac{\sum_{i=1}^{n}\sum_{j=i}^{n} abs(Ideal_{i,j} - Actual_{i,j})}{\sum_{g=1}^{gn}(gsize_g(gsize_g + 1))} \quad (8)$$

Table 1 displays the relative and absolute errors for the surveyed descriptors. It can be seen that the discrimination power of the descriptors created using spherical mapping is superior to that of the other descriptors, i.e. the error rates are significantly smaller.

Table 1. *Error-rates for the descriptors.*

Group	Descriptor	AbsErr	RelErr
Moments	Moments	4,02%	45,70%
Shape Distribution	D1	2,73%	30,98%
	D2	2,46%	27,92%
Cords	Cords	2,41%	27,34%
Spherical Mapping	SPH	1,57%	17,78%
	DWT	0,57%	6,50%

3. Conclusion

The approach presented in this paper overcomes some of the major problems in the field of matching 3D objects, the non-uniform vertex sampling and level of detail distribution, the non-uniform polygon topology and the mesh-representation anomalies by mapping an MxN sphere on the mesh-object surface.

The experimental results of the descriptors obtained using this approach show significantly greater discrimination power, compared to other descriptors.

A good feature of the proposed approach is also its scalability, that is, by working with more samples on the sphere, we should obtain closer approximations to the objects and thus, better descriptors.

Acknowledgment

This work is partially supported by the EGIDE and The French Embassy in Skopje.

References

[1] H. Alt and L. J. Guibas. “Discrete geometric shapes: Matching, interpolation, and approximation: A survey”. *Technical Report B 96-11*, EVL-1996-142, Institute of Computer Science, Freie Universitat Berlin, 1996.

[2] T. Funkhouser, P. Min, M. Kazhdan, J. Chen, A. Halderman, D. Dobkin, and D. Jacobs, “A Search Engine for 3D Models", *ACM Transactions on Graphics*, 22(1):83-105, January 2003

[3] D. Healy, D. Rockmore, P. Kostelec, and S. Moore, “FFTs for the 2-Sphere - Improvements and Variations", *Tech. Rep. TR2002-419*, Department of Computer Science, Dartmouth College, Hanover, NH, 2002

[4] M. Hilaga, Y. Shinagawa, T. Kohmura, and T. L. Kunii, “Topology Matching for Fully Automatic Similarity Estimation of 3D Shapes", *in Proc. SIGGRAPH 2001,* Los Angeles, CA, August 2001, pp. 203-212, ACM SIGGRAPH

[5] MPEG-7 Requirements Group, “*MPEG-7 Requirements Document*”, V.15. ISO/IEC N4713, MPEG-7, Sydney, July 2001

[6] MPEG-7 Video Group, “*Information Technology - Multimedia Content Description Interface - Part 3: Visual*”, ISO/IEC FCD 15938-3 / N4062, MPEG-7, Singapore, March 2001

[7] R. Osada, T. Funkhouser, B. Chazelle, , and D. Dobkin, “Matching 3D Models with Shape Distributions," in *Proc. SMI 2001*, Genova, Italy, May 2001, pp. 154-166

[8] E. Paquet and M. Rioux, “Nefertiti: a Query by Content Software for Three - Dimensional Databases Management”, *in Proc. IEEE 3-D Digital Imaging and Modelling*, Ottawa, Canada, May 1997, pp. 345-352

[9] F. Simons, “*Spherical harmonics and localization: the definitive suite*”, http://www.es.ucl.ac.uk/people/fjsimons/

[10] M. T. Suzuki, “A Web-based Retrieval System for 3D Polygonal Models”, *in Proc. Joint 9th IFSA World Congress and 20th NAFIPS International Conference (IFSA/NAFIPS2001)*, Vancouver, Canada, July 2001, pp. 2271-22

[11] I. T. Jollie, *Principal component analysis*, Springer-Verlag, 1986.

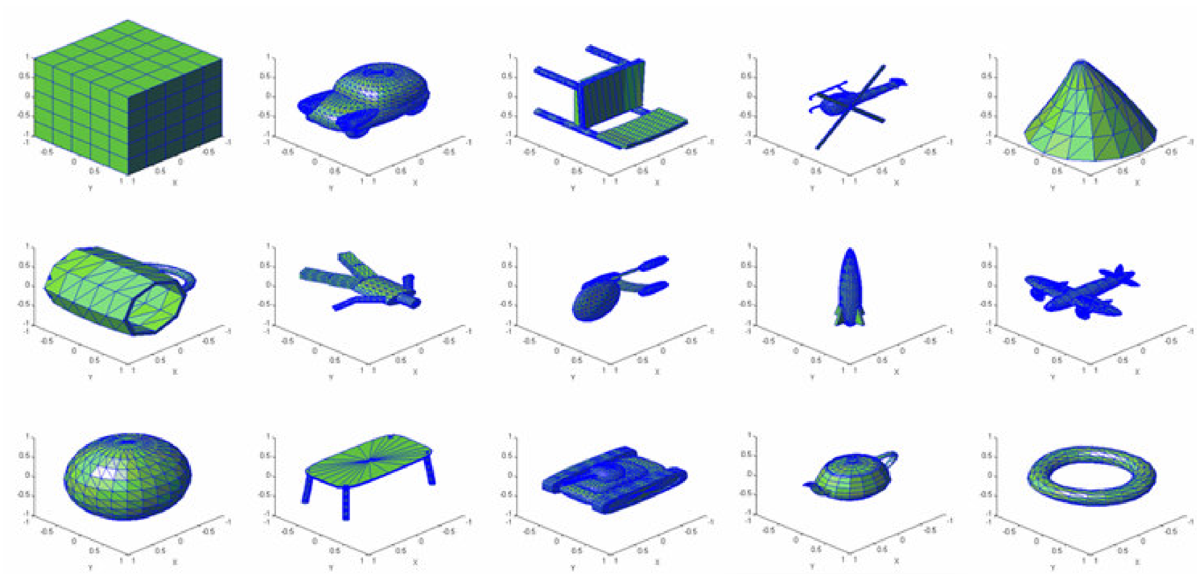

Figure 3. *Test-object groups.*

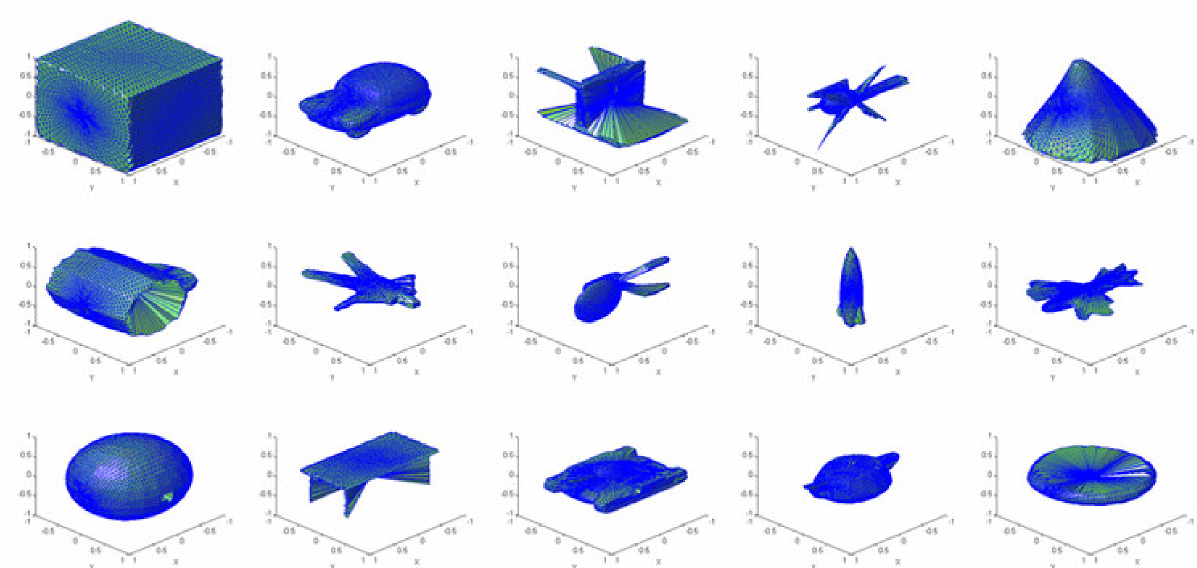

Figure 4. *Spherical approximations of the test-objects.*

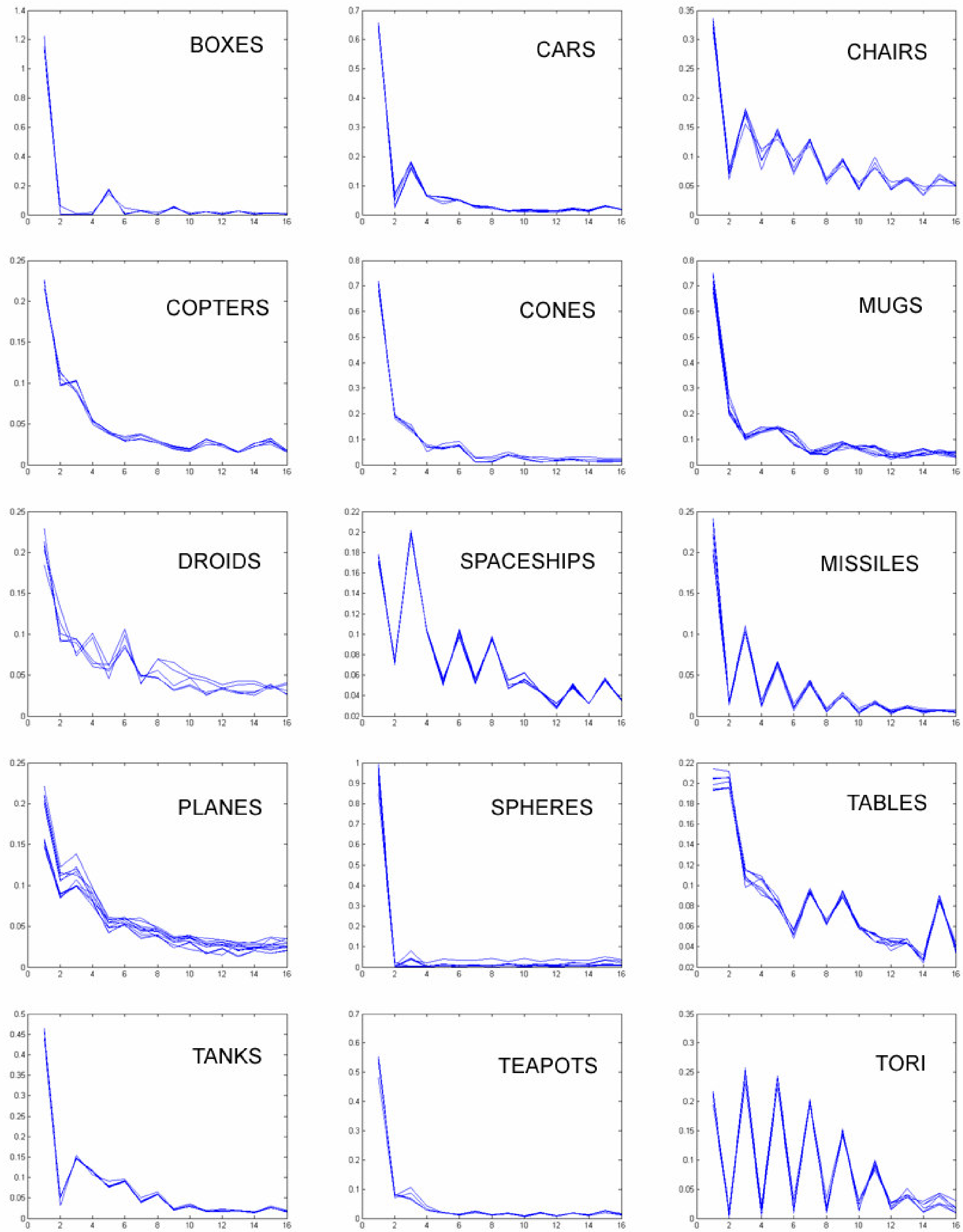

Figure 5. *Robustness test for the descriptor based on spherical harmonics.*

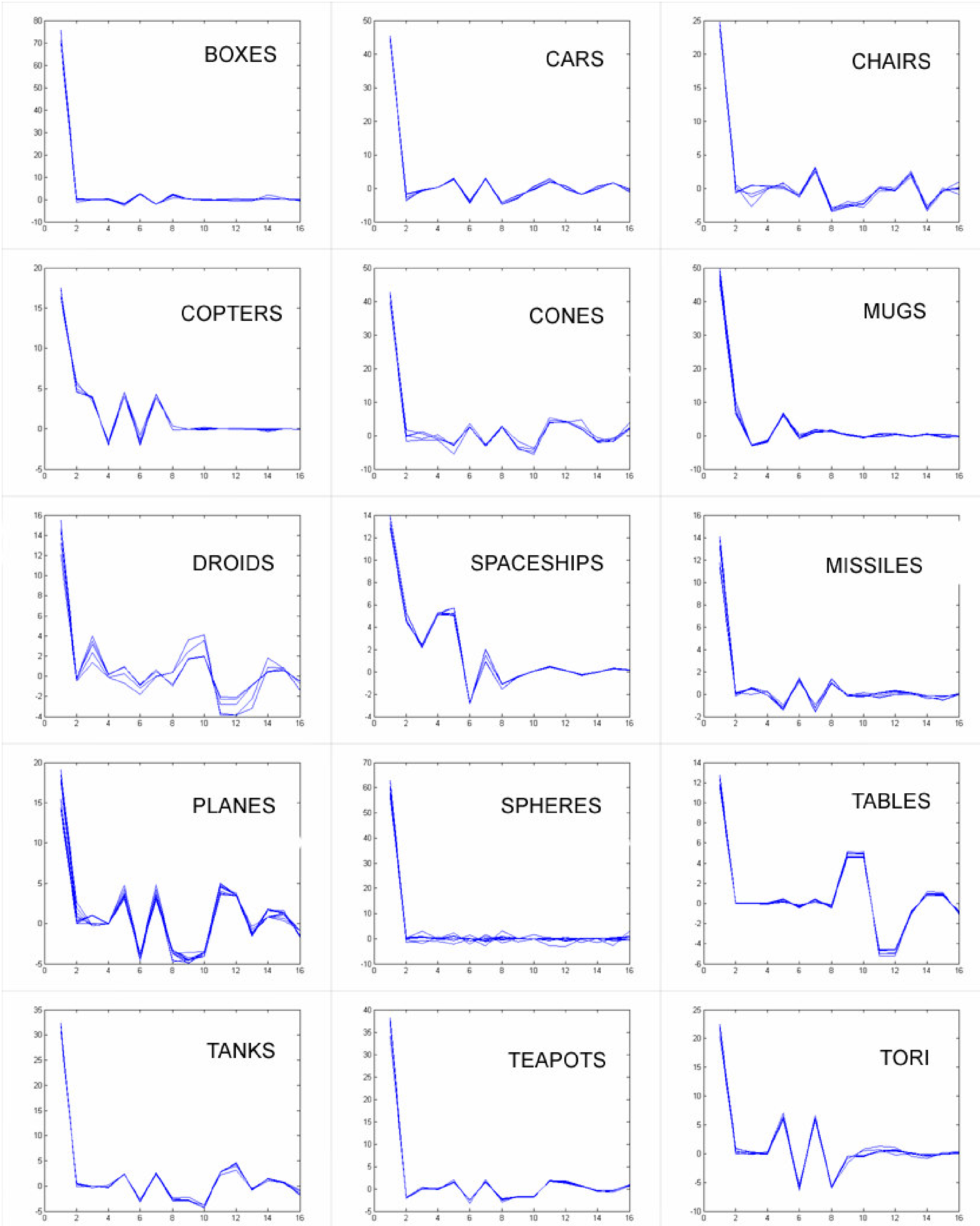

Figure 6. *Robustness test for the descriptor based on planar mapping and DWT.*

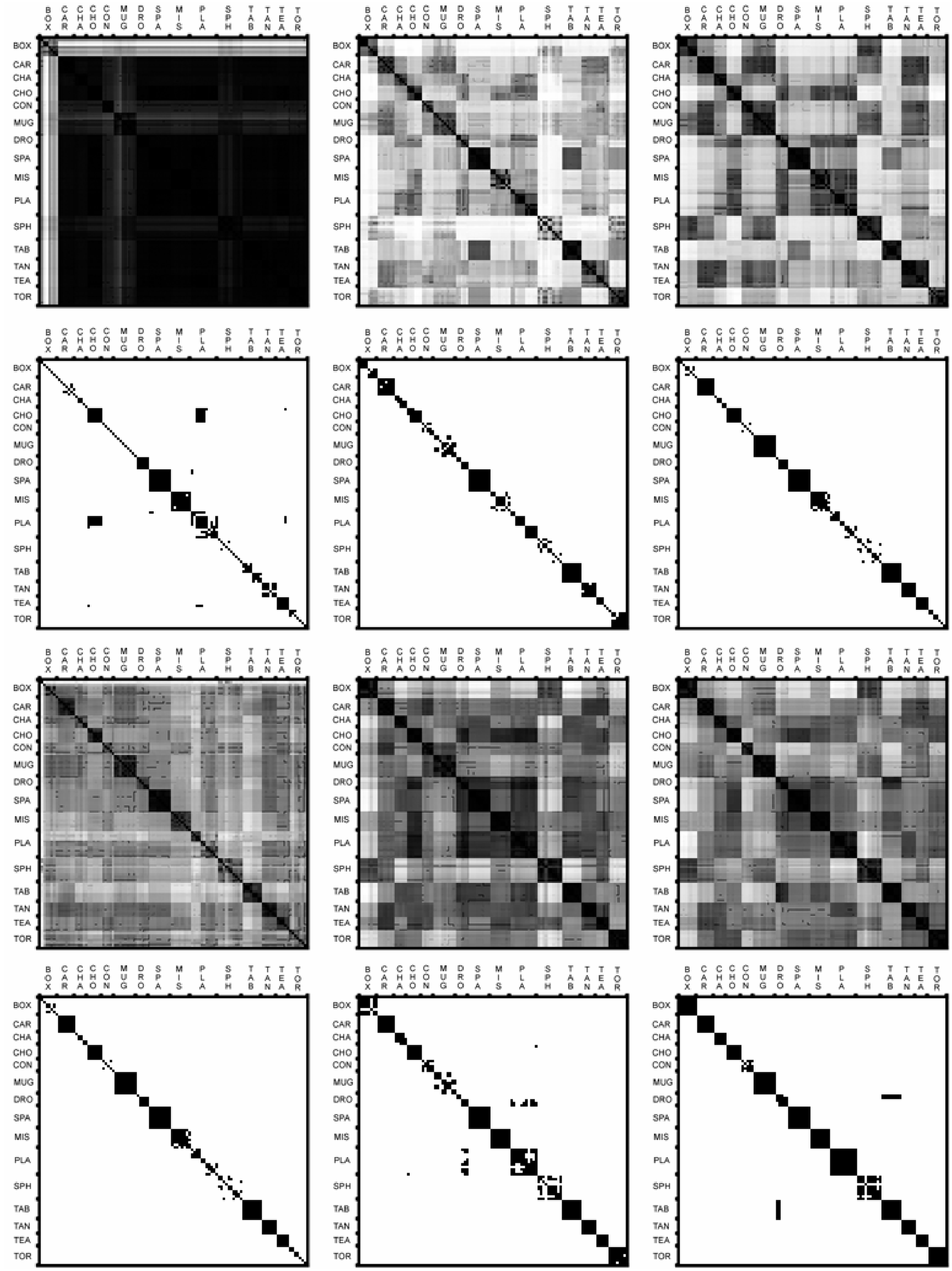

Figure 7. *Similarity matrices and their thresholded binary versions (below) for the moments based, D1 shape distribution, D2 shape distribution, cords-based and the two descriptors created with spherical mapping (using spherical harmonics and DWT).*